Available online at www.sciencedirect.com

ScienceDirect

www.elsevier.com/locate/jes

JES JOURNAL OF ENVIRONMENTAL SCIENCES

www.jesc.ac.cn

Impact of density of coating agent on antibacterial activity of silver nanoparticle impregnated plasma treated activated carbon

*Pritam Biswas, Rajdip Bandyopadhyaya**

Department of Chemical Engineering, Indian Institute of Technology Bombay, Powai, Mumbai 400076, India

ARTICLE INFO

Article history:
Received 19 May 2017
Revised 28 July 2017
Accepted 15 August 2017
Available online 30 August 2017

Keywords:
Silver nanoparticles
Activated carbon
Escherichia coli
Citrate coating
Coating density
Water disinfection

ABSTRACT

To use stabilized nanoparticles (NPs) in water as disinfectants over a very long period, the amount of coating agent (for NP stabilization) needs to be optimized. To this end, silver nanoparticles (Ag-NPs) with two different coating densities of tri-sodium citrate (12.05 and 46.17 molecules/nm^2, respectively), yet of very similar particle size (29 and 27 nm, respectively) were synthesized. Both sets of citrate capped NPs were then separately impregnated on plasma treated activated carbon (AC), with similar Ag loading of 0.8 and 0.82 wt.%, respectively. On passing contaminated water (containing 10^4 CFU *Escherichia coli*/mL of water) through a continuous flow-column packed with Ag/AC, zero cell concentration was achieved in 22 and 39 min, with Ag-NPs (impregnated on AC, named as Ag/AC) having lower and higher coating density, respectively. Therefore, even on ensuring similar Ag-NP size and loading, there is a significant difference in antibacterial performance based on citrate coating density in Ag/AC. This is observed in lower coating density case, due to both: (i) higher Ag^+ ion release from Ag-NP and (ii) stronger binding of individual Ag-NPs on AC. The latter ensures that, Ag-NP does not detach from the AC surface for a long duration. TGA-DSC shows that Ag-NPs with a low coating density bind to AC with 4.55 times higher adsorption energy, compared to Ag/AC with a high coating density, implying stronger binding. Therefore, coating density is an important parameter for achieving higher antibacterial efficacy, translating into a faster decontamination rate in experiments, over a long period of flow-column operation.

Introduction

Silver nanoparticles (Ag-NPs) are well established as one of the most efficient water disinfecting agents (Biswas and Bandyopadhyaya, 2016a, 2016b; Sondi and Salopek-Sondi, 2004). The particles are impregnated in a host matrix to prevent their aggregation and to also avoid their leaching into the environment. However, in most cases, antibacterial performance of only free NPs are tested in the batch mode (Li, 2012), whereas for water disinfection applications, it is more appropriate and essential to assess the performance in a continuous flow system.

Conventionally, different coating agents have been used for stabilizing and controlling the growth of Ag-NPs during nanoparticle synthesis and its impregnation. The effect of different coating agents like, sodium dodecyl sulfate (SDS), polyvinylpyrrolidone (PVP), polysorbate 80 (Tween 80), polyethylene glycol (PEG), citrate *etc.* in the aggregation kinetics and stability of NPs was already reported in previous works (Kvítek et al., 2008; Tejamaya et al., 2012). Tri-sodium citrate was extensively used as both a reducing and a coating agent during Ag-NP synthesis, since it is non-toxic and considered safe for drinking water applications (Biswas and Bandyopadhyaya, 2016a; Srinivasan et al., 2013). To the best of our knowledge, the effect of coating

* *Corresponding author*. E-mail: rajdip@che.iitb.ac.in (Rajdip Bandyopadhyaya).

http://dx.doi.org/10.1016/j.jes.2017.08.008
1001-0742/

density of citrate on Ag-NPs, on the antibacterial activity has not been extensively investigated.

Toxicity of Ag-NPs to bacterial cells is primarily because of the release of Ag^+ ion, *via* the dissolution of Ag-NPs (Jung et al., 2008; Li, 2012; McShan et al., 2014). Now, coating agent is used primarily for stabilizing the NPs and controlling their size during the Ag-NP synthesis. However, the coating agent also affects the surface chemistry and thereby the ion release kinetics, during cell-killing.

Therefore, in the present work, antibacterial activity of citrate coated Ag-NPs of same particle size and of same loading percentage in activated carbon (AC) (as Ag/AC), but having different coating densities of citrate have been assessed in a continuous flow-column. The performance has been evaluated in terms of both release of Ag^+ ion and detachment of Ag-NPs from the AC surface, for assessing the effect of coating density on the water disinfection performance during long term water disinfection.

1. Materials and methods

1.1. Synthesis of Ag-NPs with different coating density

For synthesizing Ag-NPs, silver nitrate ($AgNO_3$, Qualigens, India) was used as a precursor and tri-sodium citrate ($Na_3C_6H_5O_7$, $2H_2O$, Qualigens, India) as a reducing as well as capping agent. In the first method, typically, 70 mL, 0.01 mol/L $AgNO_3$ was mixed with 7 mL, 0.01 mol/L trisodium citrate and the reaction mixture was placed in a ultraviolet (UV) chamber (365 nm wavelength) for 12 hr, to form Ag-NPs (Appendix A. Fig. S1a). In the second method, 100 mL, 7 mmol/L tri-sodium citrate of pH 11.1 was prepared (adjusted by addition of NaOH) and heated at 100°C. Subsequently, 1.0 mL, 0.1 mol/L $AgNO_3$ was added dropwise to the reaction mixture and maintained at a mixing speed of 500 r/min and a temperature of 100°C for 1 hr. The color of reaction mixture changes from colorless to yellow, then turbid, indicating the completion of reaction (Appendix A. Fig. S1b).

With the aim of measuring the time required for the completion of nanoparticle formation, absorbance of NP suspension was measured using an UV–vis spectrophotometer (Lambda 35, Perkin Elmer, USA). For checking the mechanism of formation of Ag-NPs for both the Ag-NPs, time dependent imagining and measurement of particle size was performed using field emission gun-transmission electron microscopy (FEG-TEM) (JEM-2100F, JEOL, Japan) and dynamic light scattering (DLS) (Zetasizer Nano ZS, Malvern Instruments, UK). Samples were collected after 3, 6, 12 and 14 hr and 10, 30, 60 and 80 min for Ag-NP with low and high citrate coating densities, respectively. Size distribution was generated from images of Ag-NPs by measuring at least 500–600 particles from both the synthesis methods, by measuring 200 particles from each synthesis run.

1.2. Measurement of coating density of citrate for both the Ag-NPs

The synthesized Ag-NP suspension contains citrate coated Ag-NPs and excess free citrate. For ensuring complete removal of excess citrate from the Ag-NP suspension, the NP suspension was dialyzed using cellulose dialysis tubing (molecular weight cut off — 14,000, approximate pore size of 1.4 nm, Sigma, India). The 25 mm diameter dialysis tubes were filled with Ag-NP suspension and immersed in a 5 L milli-Q water container and a mixing speed of 300 r/min was maintained using a magnetic stirrer. The dialysis membrane allows permeation of excess citrate (molecular weight of 258.06 g/mol) and prevents the out flow of Ag-NPs (having average diameter of 27 and 28 nm). Mixing ensures faster removal of citrate molecules by preventing accumulation of citrate near the dialysis membrane. Initially the milli-Q water was changed after every 6 hr and subsequently, after 10 days water was changed after an interval of 12 hr (as the release of citrate molecule decreases over time). The dialysis was continued for 21 days for complete removal of all the excess citrate. Therefore, all the citrate molecules present in the suspension were adsorbed on the Ag-NPs. Subsequently, the suspension was dried at 80°C in a vacuum drier for preparing Ag-NP powder, which is suitable for further thermo gravimetric analysis (TGA) (STA 409 PS, NETZSCH, Germany).

The mass of the citrate molecules adsorbed on the Ag-NPs was measured by performing TGA (Appendix A. Fig. S2). Subsequently, the coating density (σ) of citrate on the Ag-NP was calculated using Eq. (1) (Benoit et al., 2012)

$$\sigma = \frac{\mathrm{wt.\%_{shell}} \times \rho_{core} \times \frac{4}{3}\pi {r_{core}}^3 \times N_A}{\mathrm{wt.\%_{core}} \times \mathrm{MW_{polymer}} \times 4\pi {r_{core}}^2} \quad (1)$$

where, $\mathrm{wt.\%_{shell}}$ is the relative mass of citrate (measured from TGA data), $\mathrm{wt.\%_{core}}$ is the residual mass of the pure Ag-NPs (measured from TGA data), ρ_{core} is the density of bulk silver, r_{core} is the average radius of Ag-NPs, N_A is the Avogadro's number, and $\mathrm{MW_{polymer}}$ is the molecular weight of tri-sodium citrate. The diameter of the particle was measured from multiple FEG-TEM images of Ag-NPs. The zeta potential (Zetasizer Nano ZS with zeta potential measurement cell, Malvern Instruments, UK) of both the samples was measured.

1.3. Impregnation of Ag-NPs on plasma treated activated carbon (AC)

Both the Ag-NPs were separately impregnated on plasma treated activated carbon (AC) (with a size range of 420–840 μm) by wet impregnation method. Typically, 5 g of plasma treated AC was added in 77 mL of Ag-NP (with low citrate coating density) suspension and 2.5 g of plasma treated AC was added to 100 mL of Ag-NP (with high citrate coating density). The mixture was maintained at 300 r/min overnight using a magnetic stirrer. Subsequently, both the granules were filtered using ash-less whatman filter paper (2 μm pore diameter) and dried at room temperature for its further use. The granules were imaged in FEG-SEM (JSM-7600F, JEOL, Japan). For measuring the Ag loading, the samples were immersed in concentrated nitric acid for 72 hr and the acidic samples were analyzed in an inductively coupled plasma atomic emission spectroscopy (ICP-AES) (ARCOS, SPECTRO Analytical Instruments GmbH, Germany).

1.4. Cell-killing experiments in a continuous flow-column

Batch mode cell-killing experiments were performed using 4, 6 and 8 mg/mL of hybrids (Appendix A. Section S3). Based on the contact time required in batch mode experiments the flow rate

was fixed in the continuous flow-column experiments. For performing continuous flow-column experiments, a column with 5 cm diameter and 25 cm height was packed with either of the two granules following Biswas and Bandyopadhyaya (2016a). The column shows a volumetric filling of 0.494.

Using Ag/AC with lower coating density as a packing material, 10^4 colony forming units (CFU)/mL of *Escherichia coli* K12 (MTCC 1302, Chandigarh, India) cells were passed at a flow rate of 0.66, 0.765 and 0.88 L/hr (corresponding to a contact time of 22, 19 and 16.5 min, respectively). Contaminated water was also passed through the same column packed with Ag/AC (having high citrate coating density), at a flow rate of 0.373, 0.4 and 0.44 L/hr (corresponding to contact time of 39, 36 and 33 min, respectively). The outlet water was collected after every 5 min and plated in agar plate. The agar plates were incubated at 37°C overnight for getting the cell count. The cell concentration was also quantified using fluorescence spectroscopy. The cells were stained with 4′,6-diamidino-2-phenylindole (DAPI) and propidium iodide (PI) (Invitrogen, Life Technologies, India). The concentrations of both the dyes were optimized depending on the *E. coli* cell concentration (Appendix A. Figs. S4a and b). The concentration of live cell was measured from the calibration plot (Appendix A. Fig. S5).

For assessing the long term performance of the columns packed with Ag/AC having low or high citrate coating density, the column was operated over 5 days at inlet flow rate of 0.66 L/hr and 0.373 L/hr respectively. Around 79.2 and 44.76 L of contaminated water were passed through the column packed with Ag/AC having low or high citrate coating density, respectively. The *E. coli* cell concentration was measured again by both plate count and fluorescence spectroscopy.

1.5. *Measurement of Ag concentration in a continuous flow-column*

For ensuring production of safe drinking water and long lasting performance of the hybrids Ag concentration was measured in a continuous flow-column. *E. coli* laden water was passed at a flow rate of 0.66 and 0.373 L/hr for Ag/AC with low and high citrate coating density packing, respectively. The collected samples were divided into two parts. The first set of sample was used for ICP-AES measurement (total concentration of Ag^+ ion and Ag-NPs). Concentrated nitric acid was added to all the samples for decomposing all the Ag-NPs to Ag^+ ions. The second part of sample was used for measuring the concentration of Ag^+ ions (excluding Ag-NPs) using a silver ion selective electrode (Perfection, Mettler Toledo, USA).

2. Results and discussion

2.1. *Synthesis and characterization of Ag-NPs with low and high citrate coating density*

Fig. S6a and b (in Appendix A) shows FEG-TEM images of well dispersed spherical Ag-NPs, having low and high citrate coating density, respectively. From these and similar images, particle size distributions were generated (Fig. 1a and b), using the ImageJ software for particle size measurement. A total of 500–600 particles were measured from three independent syntheses, by measuring 150–200 particles from each synthesis run. Ag-NPs with low and high citrate coating density show a mean particle diameter of 29 and 27 nm, with a standard deviation of 16 and 11 nm, respectively, implying that both samples have essentially same size distribution with similar mean and standard deviation. Therefore, this would be helpful later, in discerning the sole effect of different coating densities of these two samples, on antibacterial properties.

We have also shown a very few large particles that appear in these two types of samples (Appendix A. Fig. S6c and d), which show up as a tail in these distributions (Fig. 1a and b), although their number is not significant.

To investigate the mechanism of formation of nanoparticles and coating, time dependent FEG-TEM images were captured for both types of Ag-NP samples. Ag-NPs having low citrate coating density show increase in mean particle size from 15 to 22 to 28 to 28.3 nm after 3, 6, 12 and 14 hr. of reaction, respectively (Fig. 2a, b, d and e). The NP does not show any further growth after 12 hr of reaction time. In contrast, Ag-NPs having high citrate coating density show an increase in mean particle size from 14 to 21 to 27 to 27.5 nm after 10, 30, 60 and 80 min of reaction, respectively (Fig. 3a, b, d and e). The NP does not grow further after 60 min of reaction time. The completion of reaction was confirmed by measuring the absorbance of the Ag-NP suspension for both types of samples (Appendix A. Fig. S7a and b). The particle size distribution from DLS data (Figs. 2c and 3c) also shows a good match with the size distribution generated from TEM

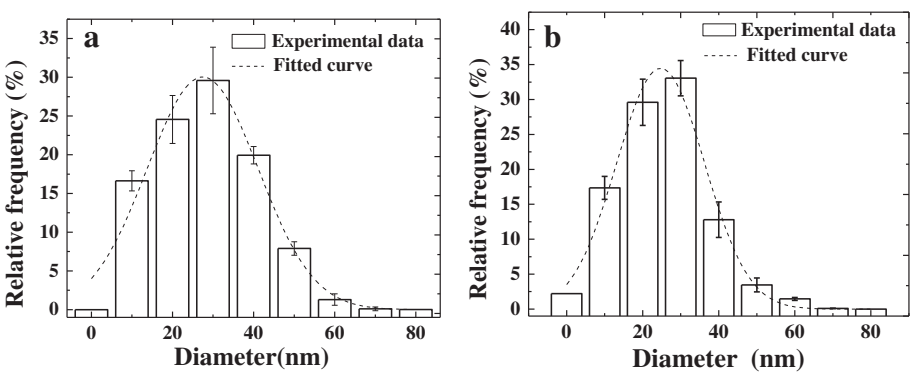

Fig. 1 – Size distribution of silver nanoparticle (Ag-NP) with (a) low and (b) high citrate coating density.

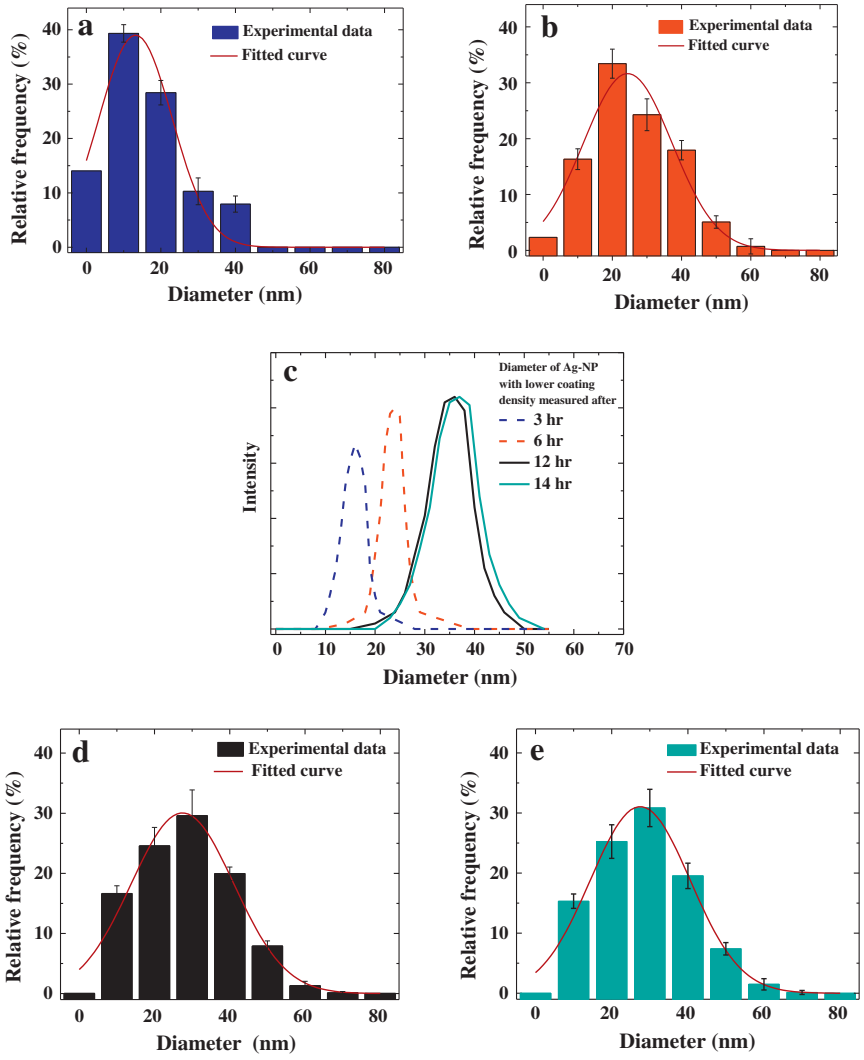

Fig. 2 – Comparison of time dependent size distribution of Ag-NPs having low citrate coating density generated from field emission gun-transmission electron microscopy (FEG-TEM) images of NPs after (a) 3, (b) 6, (d) 12 and (e) 14 hr of ultraviolet light (UV) exposure and (c) generated from dynamic light scattering (DLS) data after 3, 6, 12 and 14 hr of UV exposure.

images (Figs. 2d and 3d). Therefore, in UV reduction method the particles grow slowly over time and finally get coated with citrate. In case of Ag-NP having high citrate coating density, the particle grows faster till 30 min and subsequently gets coated with citrate and stabilizes. As the tri-sodium citrate to Ag ratio in the reaction mixture increased from 2.4 to 14.65 for Ag-NPs with low and high citrate coating density, respectively, the low coating density sample exhibits less coating density compared to the other one.

After the removal of the excess amount of free citrate from the NP dispersion *via* dialysis, TGA was performed (Appendix A. Fig. S2) and the coating densities were calculated as 12.05 and 46.17 molecules/nm^2 (with standard deviation of 0.96 and 1.06 molecules/nm^2, respectively) for high and low coting density Ag/AC samples, respectively. The coating density was quantified based on the mass loss due to removal of citrate molecules attached to the Ag-NPs during TGA. The zeta potential of both NPs with low and high coating density were −34 and −76 mV, respectively. The tail group of citrate molecule has negative charge which stabilizes the NPs. Ag-NPs with high coating show more negative zeta potential compared to NPs with low coating density, confirming the presence of more number of citrate molecules.

2.2. *Impregnation of Ag-NPs with high and low citrate coating density on plasma treated AC*

FEG-SEM image of plasma treated AC shows presence of pores all over the surface of the AC (Fig. 4a). Images of Ag/AC having low and high citrate coating density (Fig. 4b and c) shows presence of well distributed Ag-NPs all over the external surface of the AC with 0.8 and 0.82 wt.% Ag loading, respectively, given as obtained from ICP-AES measurements.

Plasma treatment ensures that: (i) more number of surface functional groups, like carbonyl, carboxylic acid *etc.* were generated on the external surface of the AC, leading to selective

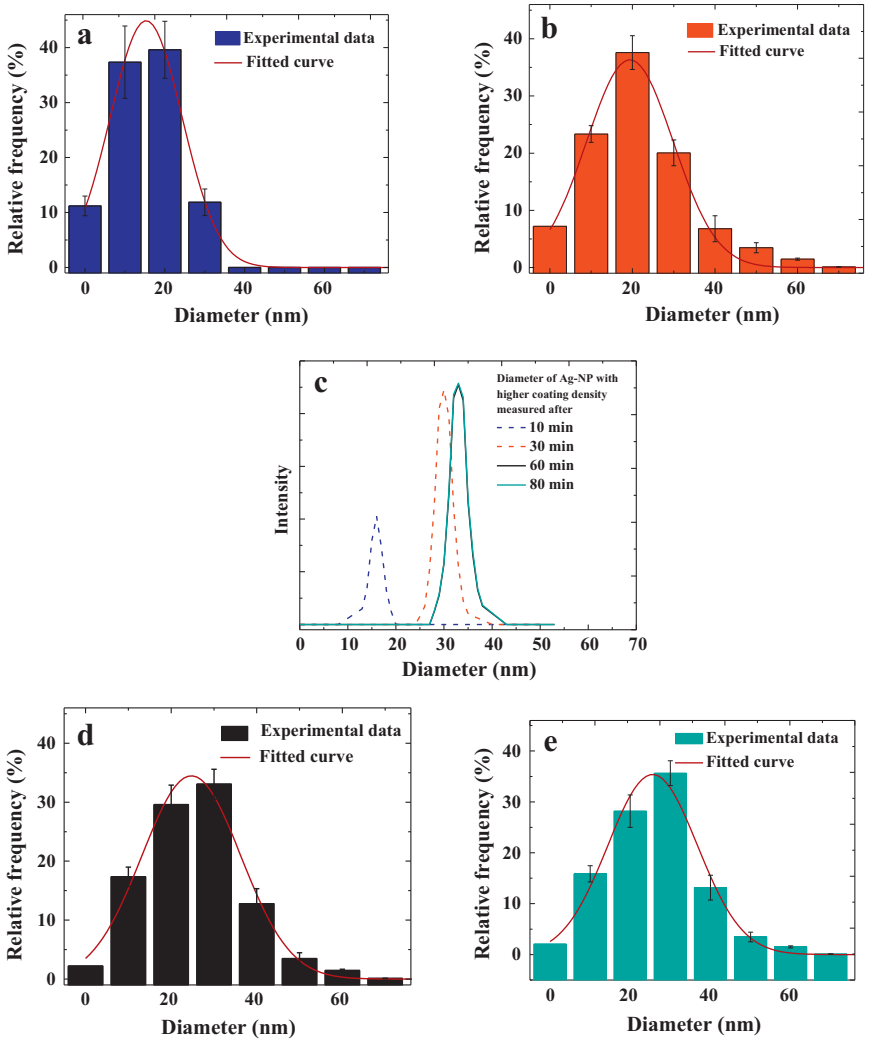

Fig. 3 – Size distribution of Ag-NP having high citrate coating density, after (a) 10, (b) 30 (d) 60 and (e) 80 min of reaction and (c) generated from DLS data after 10, 30, 60 and 80 min of reaction.

impregnation of Ag-NPs, mostly on the external surface of the AC, instead of pore interiors. This enhances the antibacterial activity of the Ag/AC granules, as the Ag-NPs present inside the pores (ranging from micro to mesopores, of far less than a micrometer diameter) are not accessible by relatively much bigger *E. coli* (1.5–2.5 μm length and 0.8–1 μm diameter, Fig. S4a (Appendix A.)) cells (Biswas and Bandyopadhyaya, 2016a); (ii) additionally, the AC surface becomes more hydrophilic leading to better wetting, thereby ensuring better contact between the *E. coli* cells and the Ag/AC surface. Finally, (iii) plasma treatment ensures generation of more number of functional groups (carboxylic acid, carbonyl *etc.*), which will bond with Ag-NPs,

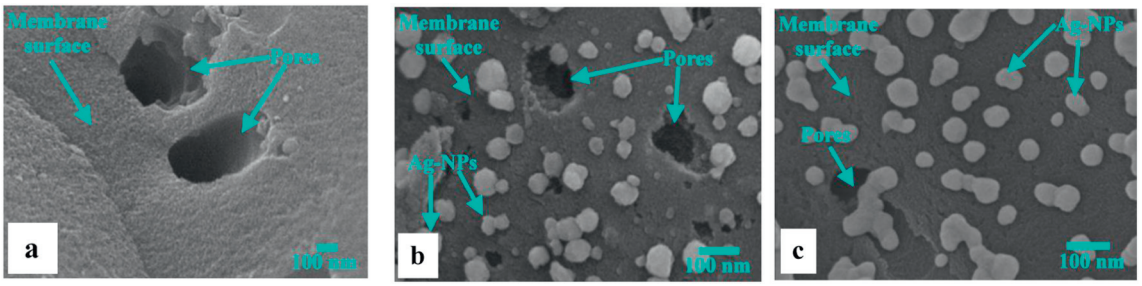

Fig. 4 – Field emission gun-scanning electron microscope (FEG-SEM) image of (a) activated carbon (AC) surface, Ag-NP impregnated AC (Ag/AC) having (b) low and (c) high citrate coating density, respectively.

resulting in much stronger attachment for ensuring minimal leaching or detachment of NPs from the AC surface during continuous flow-column experiments.

2.3. Continuous flow-column experiments with Ag/AC having low and high coating density

Based on the time required for reaching zero cell count from the batch data (Appendix A. Section S3), the flow rate of contaminated water was fixed for a 5 cm diameter column of 25 cm height. Following the same protocol as mentioned in Biswas and Bandyopadhyaya (2016a), the column was packed with Ag/AC. On passage of contaminated water with 10^4 CFU/mL of *E. coli* cells, no live cells were detected at a contact time of 22 and 39 min, for low and high citrate coating density, respectively. These contact times correspond to a flow rate of 0.66 and 0.373 L/hr, respectively (Fig. 5a and b). In both cases, on decreasing the contact time, live *E. coli* cells were detected in the outlet water. Therefore, the critical contact time of 22 and 39 min were required to ensure zero live cells in the outlet water, for Ag/AC with low and high citrate coating density, respectively. Fluorescence spectroscopy measurements for all samples show a good match with the plate count data (Appendix A. Fig. S8a and d).

During long term flow-column operation no cells were detected using Ag/AC with low coating density, even after passing 79.2 L of contaminated water over 5 days (Fig. 5c). However, with Ag/AC packing with high citrate coating density, live cells were detected, only after three days of operation (Fig. 5d). Therefore, Ag/AC having low citrate coating density is preferable over the Ag/AC with high coating density, as it kills *E. coli* faster and performs decontamination for a longer duration. Fluorescence spectroscopy measurement also leads to the same conclusion (Appendix A. Fig. S8c and d). Therefore, the coating density is observed to have a significant effect on the cell-killing performance.

The zeta potential for two different *E. coli* strains are −22 and −35 mV at pH 7.4 (Alves et al., 2010; Halder et al., 2015), respectively. At pH 7.4, the Ag-NPs with low and high coating density showed zeta potentials of −34 and −76 mV, respectively. This implies that, there will be lower electrostatic repulsive force between *E. coli* cells and the Ag/AC surface, in case of low coating density sample, due to the latter's lower zeta potential. Therefore, for the case low coating density sample, *E. coli* cells will come in contact with the Ag-NPs somewhat more easily, which will result in it achieving faster cell killing, compared to Ag/AC with higher coating density.

2.4. Measurement of concentration of Ag in outlet water from continuous flow-column

Ag concentrations in the treated water during batch mode experiments are shown in Section S.9 (Appendix A). In a continuous flow-column, on using Ag/AC with low citrate coating density packing material, the total Ag concentration (Ag-NP and Ag^+ ion) in the outlet water reaches a value of

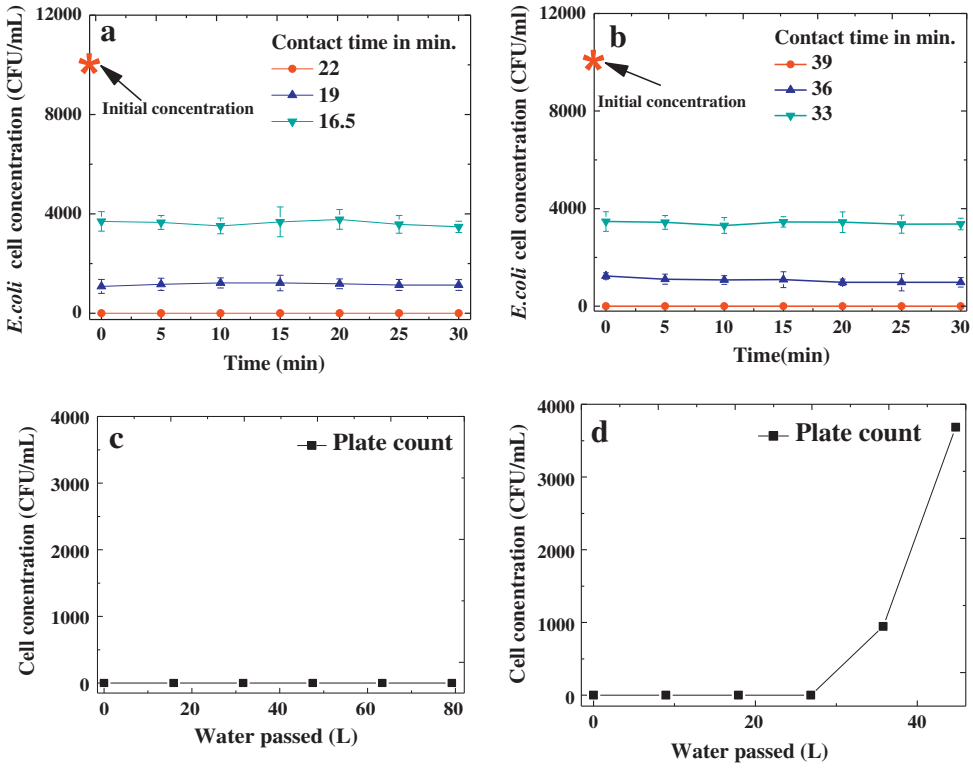

Fig. 5 – Time-dependent cell count measured by plate count method in the treated water using a 5 cm diameter column with 25 cm height, from an initial cell concentration of 10^4 CFU/mL for different contact times using Ag/AC packing with (a) low and (b) high citrate coating density packing. Long term cell-killing data measured by plate count using Ag/AC having (c) low and (d) high citrate coating density.

0.043 mg/L after 12 hr and then onwards remains almost constant for 5 days [Fig. 6], beyond which experiments were not performed. Ion selective electrode also shows Ag^+ ion concentration of 0.042 mg/L (only Ag^+ ion) for the same sample. This implies, no Ag-NPs were leaching out during the experiments and cell-killing occurred mainly due to the release of Ag^+ ions and the Ag concentration remains below the permissible limit of 0.1 mg/L (EPA, 2015; WHO, 1996). This is because, Ag/AC with low citrate coating density has an optimum coating density for stabilization of Ag-NP, better attachment of Ag-NPs on the AC surface and the release of Ag^+ ions. In a continuous flow-column only 0.5 wt.% of the total Ag loaded was released using Ag/AC having low citrate coating density after continuous uninterrupted operation of 5 days, preserving most of the Ag intact (Appendix A. Fig. S10).

In contrast, Ag/AC with high citrate coating density however shows large fluctuations in concentration of Ag in the treated outlet water. On plotting the individual experimental data during six consecutive runs, it is observed that in some of the runs (runs 4 and 5) the concentration shots up and show very high fluctuation (Appendix A. Fig. S11). Ion selective electrode shows a steady state Ag^+ ion concentration of only 0.02 mg/L, which is much below the concentration of total Ag (*i.e.*, Ag-NP and Ag^+ ion) (0.225 mg/L). Therefore, the reason behind the fluctuation of Ag concentration was detachment of Ag-NPs from the Ag/AC having high citrate coating density. Moreover, the Ag concentration crosses the permissible limit of 0.1 mg/L (EPA, 2015; WHO, 1996) for drinking water. In the long term experiment, 4.2 wt.% of the total Ag loaded was released after 5 days, using Ag/AC having high citrate coating density (Appendix A. Fig. S10).

Higher coating density affects the attachment efficiency of the Ag-NP as well as the Ag^+ ion release. This was also reflected in the long term flow-column experiment. A breakthrough in the performance of the flow-column was observed after three days itself [Fig. 5d] due to fall in release concentration of Ag^+ ions, although the total release of Ag was high due to detachment of Ag-NPs.

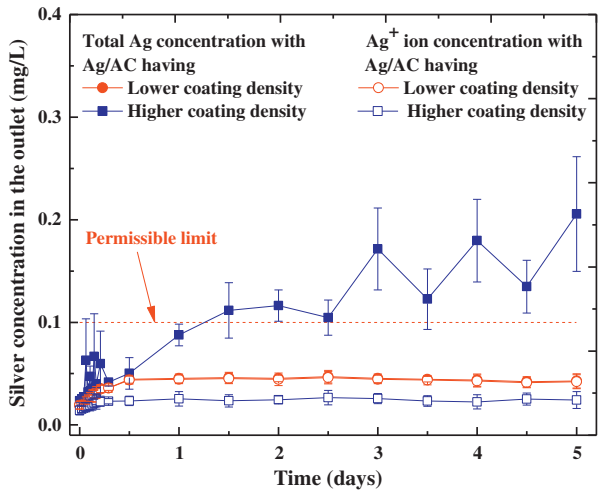

Fig. 6 – Ag concentration in the treated water collected from the flow-column (with 5 cm diameter and 25 cm height) with Ag/AC packed column with low and high citrate coating density, at a flow rate of 0.66 and 0.373 L/hr, respectively, measured by (a) inductively coupled plasma-atomic emission spectroscopy (ICP-AES) and (b) ion-selective electrode.

The attachment efficiency of Ag-NPs on the AC surface was quantified by thermogravimetry and differential scanning calorimetry (TGA-DSC) measurement (Appendix A. Fig. S12). Based on this validated method the energy of desorption were calculate and found to be 667.01 and 146.71 kJ/mol. It seems both the NPs were chemisorbed on the surface of the AC. Typically, the desorption energy of individual small single molecules ranges from 80 to 100 kJ/mol. In the present work the energy of desorption is much higher as the nanoparticles are composed of a large number of molecules, giving larger desorption energy, than single molecules. Ag/AC with low coating density shows almost 4.55 times higher adsorption energy, which confirms that these Ag-NPs were bonded much strongly with the AC surface compared to the Ag-NPs with high coating density. This results in easy detachment of Ag-NPs from the AC surface during the Ag release experiments in case Ag/AC with high coating densities.

In the present experiments, the adsorption energy of Ag-NPs on the AC surface were estimated to be 667 and 146.7 kJ/mol for low and high coating density Ag/AC granules, respectively (Appendix A. Fig. S12). Therefore, Ag-NPs with low coating density are bound more strongly to the AC surface, compared to the high coating density sample. However, for Ag/AC with low coating density, due to the lower number of citrate molecules involved, the Ag-NP surface mostly remains uncovered, which helps in better contact between the surrounding water and the Ag-NP itself, leading to a higher dissolution of Ag^+ from the Ag-NP itself. Additionally, the zeta potential of Ag-NPs with low coating density further enhances the cell killing due to reduced electrostatic repulsion with Ag/AC, thereby, resulting in a faster cell-killing. Hence, it is likely that, for low citrate coating density Ag/AC sample, the two factors of higher available surface area on Ag-NP and its lower zeta potential results in more favorable Ag^+ ion release from it, whereas, the single factor of its higher adsorption energy to AC probably shows an opposite effect. Thus, altogether we may have observed higher antibacterial effect in case of lower coating density sample.

Ag-NP attaches to the carboxylic acid and carbonyl groups present on the AC surface. In the case of Ag-NPs with higher coating density, the coating agent hinders the interaction and hampers the attachment between the Ag-NPs and surface functional groups. Therefore, Ag-NPs are loosely bound to the AC surface with weak interactions. In contrast, the Ag-NPs with lower coating density attaches well with functional groups, without much interference due to the coating agent. All these factors culminate into a higher disinfection performance of Ag/AC having low citrate coating density hybrid compared to Ag/AC having high citrate coating density hybrid. Additionally, as the concentration of Ag is much lower (0.043 mg/L) in case of Ag/AC with low coating density samples, it will exhibit antibacterial performance for a long duration compared to Ag/AC with low coating density (0.225 mg/L).

With the aim of comparing the cell killing activity of Ag/AC with that of the same amount of Ag^+ ion as a control (as released by Ag/AC in release experiments), batch mode cell killing experiments were performed with Ag/AC concentration of

4 mg/mL for (Appendix A. Section 13). On using Ag^+ ion, zero live cell concentration has been reached in 25 and 40 min, compared to 35 and 45 min, while using Ag/AC granules with low and high coating density, respectively (Appendix A. Fig. S13). In batch experiments, When Ag/AC granules were used, the initial Ag^+ concentration was zero (Appendix A. Fig. S13), whereas in control experiments there is either Ag^+ ion, which is much higher. This therefore obviously leads to a faster cell killing, compared to only Ag/AC granules (without any initial Ag^+ ions) and decreases contact time for reaching zero live cell concentration.

2.5. Comparison of rate constant with literature

Water disinfection performance of Ag-NP impregnated hybrids are compared (Table 1) with present work in terms of (1) initial *E. coli* (CFU/mL) cell concentration, (2) amount of Ag used per mL of cell suspension and (3) death rate constant (Table 1).

Altintig et al. (2016) (i) could achieve only a 8.7 times lower death rate constant, compared to the present work, although they used a very low cell concentration and that too with a very high Ag concentration, compared to the present work. Tuan et al. (2011) (ii) have reported a rate constant value of 0.9 hr^{-1}, which is 8.2 times less than the present work, since their cell concentration is higher and the amount of Ag used is lower compared to the present work. Zhao et al. (2013) (iii) and Acevedo et al. (2014), (iv) have reported almost 6.39 and 3.04 times lower death rate constant compared to the present work (vii).

This is even though in both cases, 3.03 and 4.56 times higher amount of Ag was used, respectively, albeit for higher *E. coli* cell concentration. In all other four cases in literature, as Ag-NPs were present inside pore interiors as well as on the surface, a significant amount of Ag in pore interiors was not accessible by the bacterial cells.

In contrast, in the present work, most of the Ag-NPs were selectively impregnated on the external surface of the AC, to result in a much better cell-killing performance, with a comparatively lower Ag loading. On using Ag/AC having a low citrate coating density (vii), we could achieve 2 times higher death rate constant, compared to Ag/AC having high citrate coating density (vi). Ag/AC having low citrate coating density shows higher release of Ag^+ ions, than Ag/AC having high citrate coating density. This finally results in better antibacterial activity of this hybrid.

3. Conclusions

Effect of coating density of citrate on silver nanoparticle (Ag-NP) was assessed for water disinfection. For this, Ag-NPs with different coating densities (12.05 and 46.17 molecules/nm^2 of Ag-NP surface area, termed as Ag-NPs with low and high coating density, respectively) were synthesized. These were separately impregnated in plasma treated, activated carbon (AC), and designated as Ag/AC, *i.e.*, AC containing Ag-NP. In spite of having similar NP size (mean diameter of 29 and 27 nm) and similar Ag loading (0.8 and 0.82 wt.%) in the two types of Ag/AC, they had significantly different antibacterial efficacy. It was observed that, a flow-column (of 5 cm diameter and 25 cm height) packed with Ag/AC of low coating density, could completely disinfect contaminated water (with 10^4 CFU/mL of *E. coli* cells) in only 22 min, compared to Ag/AC of high coating density, which took as much as 39 min. This is because the steady state concentration of Ag^+ ion in the treated, outlet water from the column is 0.042 mg/L for Ag/AC with low coating density, which is two times higher compared to concentration of Ag^+ ion (0.02 mg/L), for the case of high coating density. This implies that higher Ag^+ ion concentration leads to faster cell-killing and thereby, requires lower contact time for Ag/AC with low citrate coating density.

Furthermore, in the case of Ag/AC with low coating density, the concentration of only Ag^+ ion is almost same as the total concentration of Ag, consisting of Ag in both NP and ionic form. This implies that, Ag was released only as Ag^+ ions and there is no detachment of Ag-NPs. In contrast, Ag/AC with high citrate coating density shows significantly higher (0.225 mg/L) overall Ag release (combining Ag^+ ion and Ag-NP), confirming detachment of Ag-NPs. In fact, TGA-DSC measurement shows that the Ag-NPs with low coating density binds to AC with an adsorption energy of 667.01 kJ/mol, which is 4.55 times higher compared to

Table 1 – Comparison of rate constant with previous work, for batch mode *Escherichia coli* (*E. coli*) cell-killing using silver nanoparticle impregnated activated carbon (Ag/AC). The rate constant values from the present work being highest, are highlighted in bold.

Serial No.	Cell concentration (CFU/mL)	Amount of silver per mL of cell suspension (mg/mL)	Rate constant (hr^{-1})	References
(i)	200	1.675 [a]	0.85 [b]	Altintig et al. (2016)
(ii)	10^6	0.02 [a]	0.90 [b]	Tuan et al. (2011)
(iii)	10^7	0.194 [a]	1.16 [b]	Zhao et al. (2013)
(iv)	10^7	0.292 [a]	2.44 [b]	Acevedo et al. (2014)
(v)	10^7	0.354 [a]	2.62 [b]	Acevedo et al. (2014)
(vi)	**10^4**	**0.064**	**3.68** [c]	Present work (Ag/AC with high citrate coating density)
(vii)	**10^4**	**0.064**	**7.41**	Present work (Ag/AC with low citrate coating density) and Biswas and Bandyopadhyaya (2016a)

[a] Concentration of Ag per mL of cell suspension was calculated from the concentration of Ag/AC used (mg/mL of water) and Ag loading in the Ag/AC hybrid (wt.%).
[b] Rate constant values were calculated based on the cell concentration *versus* time data provided in the literature.
[c] Representative plot with fitted curve for determination of death rate constant value using 8 mg/mL of Ag/AC having high citrate coating density was shown in Appendix A. Fig. S14.

Ag/AC with high coating density, for which the adsorption energy is only 146.71 kJ/mol. This results in detachment of Ag-NPs from Ag/AC with high coating density. In contrast, for Ag/AC with low coating density, the Ag-NP is strongly bound to the AC surface, which will ensure no Ag-NP loss and hence cell-killing for a very long duration.

Therefore, important findings of the present work are: (i) lower coating density of citrate on NPs leads to higher antibacterial activity due to higher ion release and also (ii) lower coating density of citrate increases the attachment efficiency of Ag-NPs on the AC surface, preventing any detachment of Ag-NPs during continuous-flow operation. Hence, low coating density is favorable for achieving maximum water disinfection efficiency and ensures a long lasting performance with Ag concentration within the permissible limit for drinking water.

Acknowledgments

We thank the Department of Chemical Engineering, Indian Institute of Technology (IIT Bombay) for providing FEG-SEM and TGA-DSC facilities. We also thank sophisticated analytical instrumental facility (SAIF), IIT Bombay for FEG-TEM, FEG-SEM and ICP-AES.

Appendix A. Supplementary data

Supplementary data to this article can be found online at http://dx.doi.org/10.1016/j.jes.2017.08.008.

REFERENCES

Acevedo, S., Arevalo-Fester, J., Galicia, L., Atencio, R., Plaza, E., Gonzalez, E., 2014. Efficiency study of silver nanoparticles (AgNPs) supported on granular activated carbon against *Escherichia coli*. J. Nanomedicine Res. 1, 4–8.

Altintig, E., Arabaci, G., Altundag, H., 2016. Preparation and characterization of the antibacterial efficiency of silver loaded activated carbon from corncobs. Surf. Coat. Technol. 304, 63–67.

Alves, C.S., Melo, M.N., Franquelim, H.G., Ferre, R., Planas, M., Feliu, L., et al., 2010. *Escherichia coli* cell surface perturbation and disruption induced by antimicrobial peptides BP100 and pepR. J. Biol. Chem. 285, 27536–27544.

Benoit, D.N., Zhu, H., Lilierose, M.H., Verm, R.A., Ali, N., Morrison, A.N., et al., 2012. Measuring the grafting density of nanoparticles in solution by analytical ultracentrifugation and total organic carbon analysis. Anal. Chem. 84, 9238–9245.

Biswas, P., Bandyopadhyaya, R., 2016a. Water disinfection using silver nanoparticle impregnated activated carbon: *E. coli* cell-killing in batch and continuous packed column operation over a long duration. Water Res. 100, 105–115.

Biswas, P., Bandyopadhyaya, R., 2016b. Biofouling prevention using silver nanoparticle impregnated polyethersulfone (PES) membrane: *E. coli* cell-killing in a continuous cross-flow membrane module. J. Colloid Interface Sci. 491, 13–26.

EPA, 2015. Secondary Drinking Water Standards: Guidance for Nuisance Chemicals.

Halder, S., Yadav, K.K., Sarkar, R., Mukherjee, S., Saha, P., Haldar, S., et al., 2015. Alteration of zeta potential and membrane permeability in bacteria: a study with cationic agents. Springerplus 4, 672.

Jung, W.K., Koo, H.C., Kim, K.W., Shin, S., Kim, S.H., Park, Y.H., 2008. Antibacterial activity and mechanism of action of the silver ion in *Staphylococcus aureus* and *Escherichia coli*. Appl. Environ. Microbiol. 74, 2171–2178.

Kvítek, L., Panáček, A., Soukupová, J., Kolář, M., Večeřová, R., Prucek, R., et al., 2008. Effect of surfactants and polymers on stability and antibacterial activity of silver nanoparticles (NPs). J. Phys. Chem. C 112, 5825–5834.

Li, X., 2012. Aggregation kinetics and dissolution of coated silver nanoparticles. Langmuir 28, 1095–1104.

McShan, D., Ray, P.C., Yu, H., 2014. Molecular toxicity mechanism of nanosilver. J. Food Drug Anal. 22, 116–127.

Sondi, I., Salopek-Sondi, B., 2004. Silver nanoparticles as antimicrobial agent: a case study on *E. coli* as a model for gram-negative bacteria. J. Colloid Interface Sci. 275, 177–182.

Srinivasan, N.R., Shankar, P.A., Bandyopadhyaya, R., 2013. Plasma treated activated carbon impregnated with silver nanoparticles for improved antibacterial effect in water disinfection. Carbon N. Y. 57, 1–10.

Tejamaya, M., Römer, I., Merrifield, R.C., Lead, J.R., 2012. Stability of citrate, PVP, and PEG coated silver nanoparticles in ecotoxicology media. Environ. Sci. Technol. 46, 7011–7017.

Tuan, T.Q., Son, N. Van, Dung, H.T.K., Luong, N.H., Thuy, B.T., Anh, N.T. Van, et al., 2011. Preparation and properties of silver nanoparticles loaded in activated carbon for biological and environmental applications. J. Hazard. Mater. 192, 1321–1329.

WHO, 1996. Silver in drinking-water. Guidel. Drink. Qual. 2, pp. 1–9.

Zhao, Y., Wang, Z.Q., Zhao, X., Li, W., Liu, S.X., 2013. Antibacterial action of silver-doped activated carbon prepared by vacuum impregnation. Appl. Surf. Sci. 266, 67–72.